Measurement and Characterization of the Periclase Crystal Size in Products of the Magnesite Industry and in Sintered Magnesia

Harald Harmuth, Radenthein

The importance of the periclase crystal size as a characteristic property of sintered magnesia is even growing since enhanced crystal size has shown to increase durability in many practical applications. For the measurement of the periclase crystal size lineal analysis of polished sections can be applied. Based on that measurement a specification of the crystal size by a mean characteristic value (e. g. mean diameter) is possible. Moreover the crystal size distribution can be of interest. A precondition for the calculation of the size distribution is the knowledge of the chord length distribution as it can be determined by lineal analysis. Based on this chord length distribution the distribution of the periclase crystal size can be calculated. Various size distributions exist, depending on the fraction (e. g. volume fraction, area fraction) that is in relation to the size interval. Some errors in measurement can be detected by a critical examination of the chord length distribution.

Messung und Charakterisierung der Periklaskristallgrößen in Grundstoffen und Produkten der Magnesitindustrie

Seit der vielfachen Praxisbewährung von Sintermagnesiten mit höherer Periklaskristallgröße hat sich ihre Bedeutung als Kennwert noch erhöht. Für die Bestimmung der Periklaskristallgröße kann die Linearanalyse angewendet werden. Damit ist es möglich, eine mittlere Kennzahl (z. B. einen mittleren Durchmesser) anzugeben. Darüber hinaus kann auch die Kristallgrößenverteilung von Interesse sein. Voraussetzung für ihre Berechnung ist die Kenntnis der Sehnenlängenverteilung, wie sie mit der Linearanalyse bestimmt werden kann. Damit kann die Periklaskristallgrößenverteilung berechnet werden. Es gibt mehrere Größenverteilungen, je nachdem, welcher Anteil (z. B. Volumsanteil, Flächenanteil) der Größe zugeordnet wird. Einige mögliche Meßfehler können durch eine kritische Prüfung der Sehnenlängenverteilung erkannt werden.

Mesure et détermination des caractéristiques de grosseur des cristaux de périclase des matières premières et des produits finis de l'industrie de la magnésie

Depuis que les magnésies frittées à base de périclase à grands cristaux ont donné de nombreux résultats positifs dans la pratique, cette dimension a pris encore plus d'importance en tant que caractéristique. Pour déterminer la grosseur des cristaux de périclase on peut utiliser l'analyse linéaire. Il devient ainsi possible d'indiquer une grandeur moyenne (par exemple le diamètre moyen). De plus, il peut être intéressant de connaître la distribution de la grosseur des cristaux. Pour ce calcul il est indispensable de connaître la distribution de la longueur des bordures, celle-ci pouvant être déterminée au moyen de l'analyse linéaire. Il existe plusieurs distributions de grosseur, selon la proportion (par exemple proportion de volume, proportion de surface) qui dépend de la grosseur. Certaines erreurs de mesures possibles peuvent être mises en évidence au moyen d'un examen critique de la distribution des longueurs de bordures.

1. Introduction

The periclase crystal size is an important property of sintered magnesia. Especially since the application of sintered magnesia with enhanced crystal size its determination is a necessary tool for production, quality control and development. For that purpose microscopical methods of measurement based on the reflected light microscopy of polished sections are used. A great variety of methods exists. This paper deals only with one out of these, the lineal analysis, including the evaluation of the measurements. Lineal analysis has been chosen out of two reasons: On the one hand it enables to simply specify the periclase crystal size by a mean characteristic value (e. g. a mean diameter), on the other hand it implies the possibility of the determination of the size distribution.

2. Microscopical investigation of polished sections by the help of lineal analysis

The aim of lineal analysis is to get quantitative informations about the three dimensional micro-

structure out of the investigation of a two dimensional image. The method is based on the measurement of intercepted lengths along randomly applied straight lines across the microstructure. This scanning can e.g. be done by moving the polished section of the sample relatively to the objective of the microscope. During this movement the centre of the reticle cuts the boundaries of the periclase crystals and the second phase, and imaginary chords in these phases are generated (2), (3). In dependence on the desired evaluation two different methods of measurement are possible:

(i) In the most simple case only the total length of all chords of the phase under examination and the number of these chords will be determined. If the volume fraction of that phase is of interest, the total length of the scanning line will be determined, too. In the case that the sintered magnesia is very pure and contains no second phase it is sufficient to measure the total length of the scanning line and count the number of all chords.

(ii) A fundamental information for all calculations of crystal size distribution is the chord length distribution. If the knowledge of the crystal size distribution is desired all individual chords have to be measured.

A schematic drawing of the principle of lineal analysis shows fig. 1.

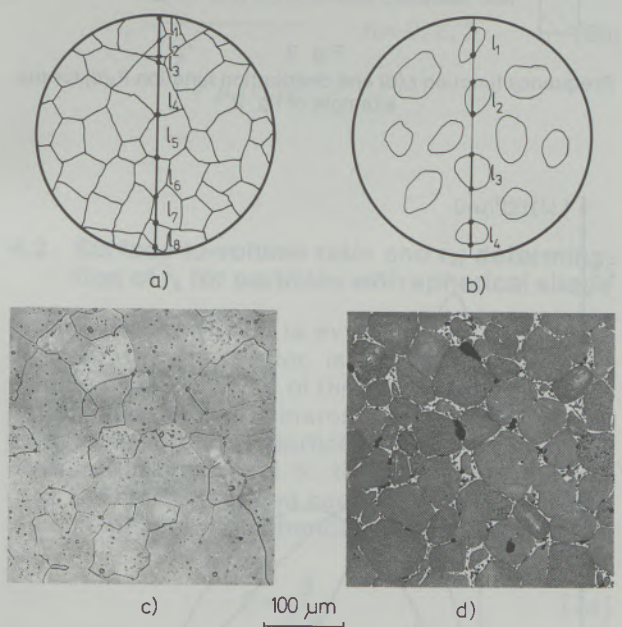

Fig. 1
Microscopical determination of the chord length using polished sections

a) one phase only (schematically)
b) phase dispersed in a matrix (schematically)
c) pure sintered magnesia (sea-water magnesia) without any second phase detectable by light microscopy
d) sintered magnesia (iron-rich natural magnesite); second phases are dicalciumferrite (bright) surrounding dicalciumsilicate (small grey particles)

Steinwender (1) reports about a computer aided microscopical measuring device that is applicable in both cases (i) and (ii). In the following part the methods of measurement and evaluation will be discussed in detail.

3. Results of the lineal analysis that are not dependent on the crystal size distribution and the crystal shape

Some fundamental results of lineal analysis are not dependent on the shape and the size distribution of the crystals, i. e. no assumptions about these attributes are necessary. These results are:

(i) The volume fraction of any phase

The volume fraction of any phase relative to the total sample volume can be approximated by the ratio of the sum of all chord lengths within this phase to the total length of the traverse within the sample. The accuracy rises when the part of the sample volume that is investigated by this method increases.

(ii) The surface-to-volume ratio

The surface-to-volume ratio S_α of a phase α is the ratio of the total area of all faces of the crystals of α to the volume of the sample. It can be calculated with the help of the mean chord length $\bar{l}_\alpha$ of α, that is the quotient of the sum of the lengths of all chords within α and the number of these chords within α.

If α is the only phase present, then

$$S_\alpha = S = \frac{2}{\bar{l}_\alpha} \qquad [1a]$$

is valid. If α is dispersed in a matrix phase, then

$$S_\alpha = \frac{4}{\bar{l}_\alpha} \qquad [1b]$$

holds. In the following parts the subscript α will be omitted for simplicity. It is of importance for the calculation of a mean crystal diameter by the help of the mean chord length that the equations [1a] and [1b] are not dependent on the size distribution of the crystals (they are not dependent on the crystal shape, too). This will be shown later.

4. Results of the lineal analysis that are dependent on the crystal size distribution and the crystal shape

4.1. Definition of the size distribution and mean characteristic values

As a rule a mean diameter (or a mean radius) is used to represent the crystal size or a particle size by a mean characteristic value. This can favourably be done when the crystal shape can be approximated by a sphere. In the case of periclase crystals this approximation is reasonable – at least when the amount of a second phase is not

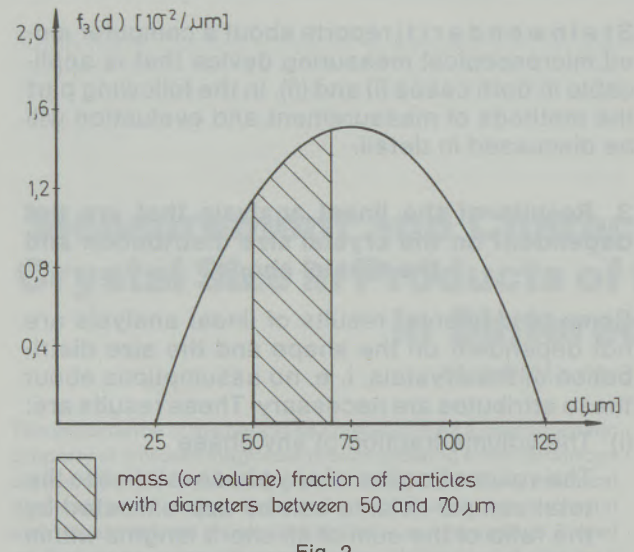

Fig. 2
Example for a frequency function specifying a particle size distribution

too small – due to the idiomorphic shape of the crystals.

The term "mean value" is not without any ambiguity unless it is specified which of the existing different definitions is used. The arithmetic and the geometric mean of the diameter of the existing particles of any phase (weighted by the number of particles) is commonly not used because it does not correlate with any given property of the structure or the material. The harmonic mean has some significance because it can be used to correlate with specific surface areas (2). The mean diameters used in this paper are defined as expected values of the diameter with respect to certain size distributions. The term "size distribution" denotes a relation of a fraction or a frequency ratio to a value that characterizes the particle or crystal size (e.g. diameter or radius). The exact specification of a size distribution can be done by one of two functions that are defined in accordance with the corresponding functions in mathematical statistics. These functions are the distribution function and the frequency function. The distribution function $F_n(r_o)$ equals a fraction that is due to particles with a radius of less of equal r_o. This fraction can be a mass or volume fraction, a surface area fraction or the relative frequency of particles. In this paper the subscript n = 0 specifies the relative frequency of particles, n = 2 the surface area fraction and n = 3 the mass or volume fraction; $F_n(r_o)$ will not be used here for the subscript n = 1. The frequency function $f_n(r)$ is the first derivative of the distribution function with respect to the radius r:

$$f_n(r) = \frac{d}{dr} F_n(r) \qquad n = 0, 2, 3 \qquad [2]$$

That implies that

$$F_n(r_1) - F_n(r_0) = \int_{r_0}^{r_1} f_n(r)\, dr \qquad n = 0, 2, 3 \qquad [3]$$

is the fraction due to particles with a radius larger than r_o and less or equal r_1. Fig. 2, 3 and 4 show examples of frequency functions and distribution functions for the same arbitrary chosen size distribution. For some of the following calculations a function $\mu(r)$ is necessary. It equals the product of

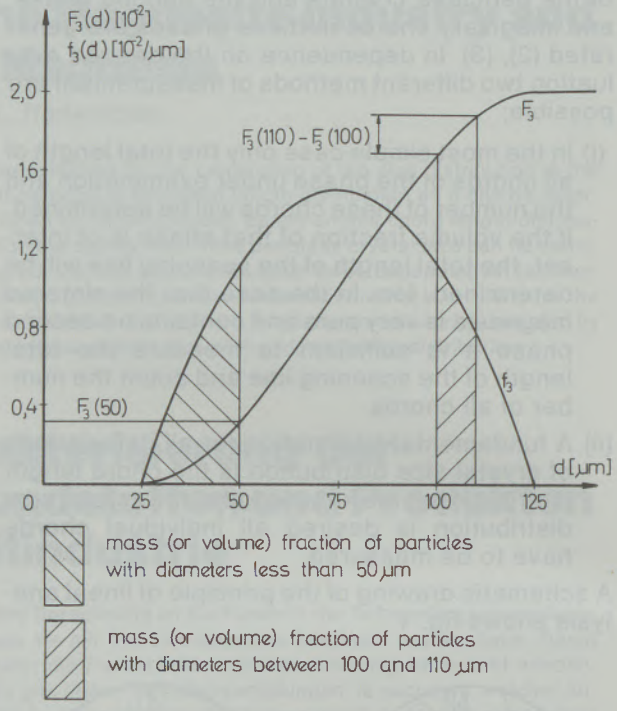

Fig. 3
Frequency function $f_3(d)$ and distribution function $F_3(d)$ for the example of fig. 2

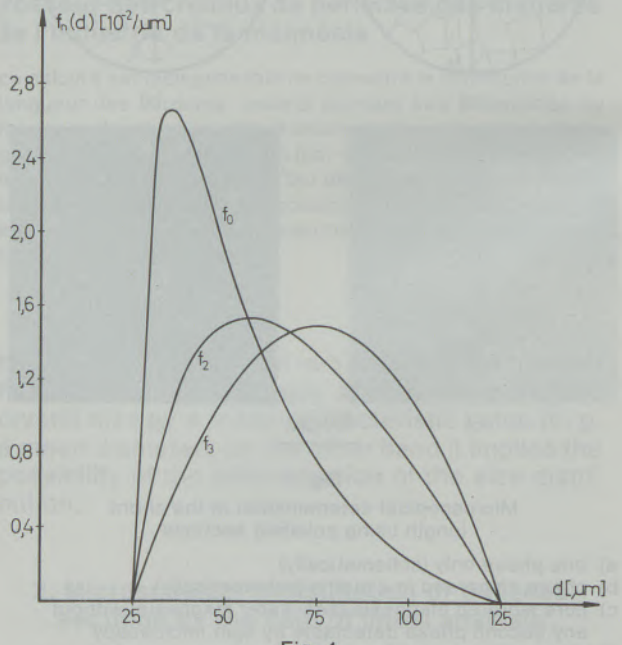

Fig. 4
Comparison of the frequency functions $f_o(d)$, $f_2(d)$ and $f_3(d)$ calculated for the size distribution of fig. 2, 3

the frequency function $f_o(r)$ and the total number of particles per unit volume. Therefore

$$N\Big|_{r_0 < r \le r_1} = \int_{r_0}^{r_1} \mu(r)\, dr \qquad [4]$$

is the number of particles with the specified radius per unit volume. With known $\mu(r)$ the frequency function $f_n(r)$ can be calculated using

$$f_n(r) = \frac{\mu(r)\, r^n}{\int_{r_{min}}^{r_{max}} \mu(r)\, r^n dr} \qquad n = 0, 2, 3 \qquad [5]$$

The smallest and the largest existing particle radius are denoted by r_{min} and r_{max}, respectively. The mean radii $\bar{r}_n$ are defined in accordance with the expected value in mathematical statistics:

$$\bar{r}_n = \int_{r_{min}}^{r_{max}} r\, f_n(r)\, dr \qquad n = 0, 2, 3 \qquad [6a]$$

or using [5] and [6a]

$$\bar{r}_n = \frac{\int_{r_{min}}^{r_{max}} r^{n+1} \mu(r)\, dr}{\int_{r_{min}}^{r_{max}} r^n \mu(r)\, dr} \qquad n = 0, 2, 3 \qquad [6b]$$

4.2. Surface-to-volume ratio and $\bar{r}_2$; determination of $\bar{r}_2$ for particles with spherical shape

From equation [6b] it is evident that in the case of n=2 the numerator is proportional to the volume of all particles of the phase under examination, and the denominator is proportional to the surface area of the particles. That is why $\bar{r}_2$ is inversely proportional to the surface-to-volume ratio S. Often S is called specific surface, too. For a single phase with spherical particles [6b] leads to

$$S = \frac{3}{2\bar{r}_2} \qquad [7a]$$

and for a dispersed phase in a matrix the specific surface can be calculated from

$$S = \frac{3}{\bar{r}_2} \qquad [7b]$$

The equations [7a] and [7b] show the importance of $\bar{r}_2$ for the determination of the periclase crystal size. In many applications of basic refractories wear is caused by a solving attack on the magnesia that starts on the surface of the periclase crystals. In this case it is therefore of great interest to lower the specific surface. The equations [7a] and [7b] show that $\bar{r}_2$ is a good indicator for the specific surface because it is inversely proportional to it.

Combination of [1a] with [7a] and [1b] with [7b] leads for a single phase and a phase dispersed in a matrix to the same result:

$$\bar{r}_2 = \frac{3}{4}\bar{l}; \quad \bar{d}_2 = \frac{3}{2}\bar{l} \qquad [8]$$

Equation [8] shows that the mean radius $\bar{r}_2$ and the mean diameter $\bar{d}_2$ of spherical particles can unambiguously be determined from the mean chord length $\bar{l}$ without any knowledge about the size distribution, because $\bar{l}$ does not depend on the size distribution (cf. section 3). This is not valid for $\bar{r}_o$ and $\bar{r}_3$ in the same way.

4.3. Determination of distributions

4.3.1. Fundamentals

The determination of a crystal or particle size distribution is in most cases based on the assumption of spherical shape (5), (6), (7), (8). This assumption is used in this work, too. For the calculation of the particle size distribution informations about the distribution function $F_z(z)$ of the chord length z or about the corresponding frequency function $f_z(z)$ are necessary. To obtain these informations the length of each individual chord can be measured with the device described in (1). Then the chord length distribution can be specified by a histogram. The following fundamentals are the background for the calculation of the

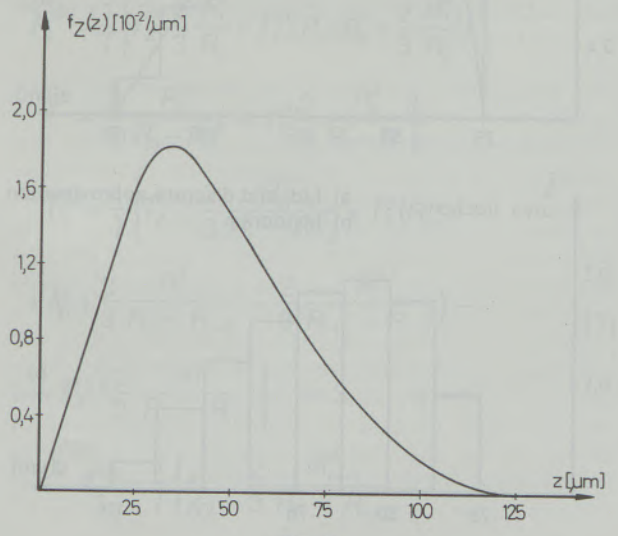

Fig. 5
Frequency function $f_z(z)$ of the chord length distribution calculated for the example of fig. 2 and 3

particle size distribution when this histogram is known.

For spherical particles the validity of the equation

$$F_Z(z) = \frac{\int_{r_{min}}^{\frac{z}{2}} r^2 \mu(r)\, dr + \frac{1}{4} z^2 \int_{\frac{z}{2}}^{r_{max}} \mu(r)\, dr}{\int_{r_{min}}^{r_{max}} r^2 \mu(r)\, dr} \qquad [9]$$

can be shown.

The first derivative is the frequency function:

$$f_Z(z) = \frac{z \int_{\frac{z}{2}}^{r_{max}} \mu(r)\, dr}{2 \int_{r_{min}}^{r_{max}} r^2 \mu(r)\, dr} \qquad [10]$$

Fig. 5 shows $f_Z(z)$ calculated for the example of fig. 2 using [10].

The equation [10] is similar to some identities of the papers cited above and it can be shown that they are equivalent. Based on these identities usually the number of particles in each diameter interval per unit volume is calculated. For that purpose the first derivative of a function characterizing the chord length distribution is often approximated by numerical differentiation. Such a method is applied by Richter (8) and he shows, that two equations of Spektor (9) and Bockstiegel (10) for calculation of the size distribution can be deduced in this way. Richter (8) also studies the erros of the method of Bockstiegel (10) and recommends measures to reduce it. Tomandl (7) describes a different method. He uses an expansion of the frequency function of the chord length distribution in a series of functions which are called invariant functions. This method does not demand any numerical differentiation. The result is the frequency function of the distribution of the diameter corresponding with $f_o(d)$; it enables to calculate the number of particles within each diameter interval.

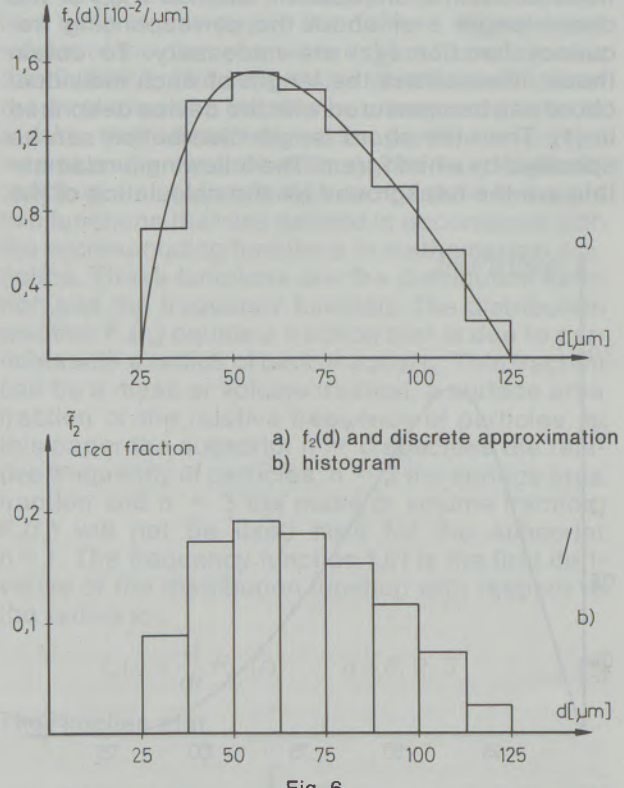

Fig. 6
Description and approximation of $f_2(d)$ calculated for the example of fig. 2, 3 and 4

Because of the considerations of section 4.2. informations about the number of periclase crystals in a certain size interval are not of primary importance. These informations are equivalent to the knowledge of the frequency function $f_o(r)$ (cf. equation [5]). Often the mean radius $\bar{r}_2$ or the mean diameter $\bar{d}_2$ are used because they are relevant to the specific surface. Therefore it seems to be more reasonable to calculate the frequency function $f_2(r)$. This function characterizes the area fraction of each size interval. Moreover it can be useful to calculate the mass or volume fraction of size intervals in accordance to the granulometry of bulk materials. This is equivalent to the knowledge of $f_3(r)$. Out of these reasons mathematical methods for the calculation of $f_2(r)$ and $f_3(r)$ have been developed during the work described in this paper. They will be explained in the following sections.

4.3.2. Determination of the distribution that is characterizing the area fraction (frequency function $f_2(r)$)

The aim is to calculate a discrete approximation of f_2 or a histogram as it is shown in fig. 6 for the example of fig. 2 and 3.

Using [9] and [10] the simple equation

$$F_Z(z) - \frac{z}{2} f_Z(z) = F_2\left(\frac{z}{2}\right) \qquad [11]$$

can be deduced. A discretization of the chord length z is used. Fig. 7 shows a schematic drawing of a histogram. The limits of the intervals are labeled $2R_i$ because they are chosen as the diameters of the size distribution too. It is not necessary that they are arranged equidistantly. The number of intervals is n. The symbol $\tilde{f}^{(i)}$ stands for the fraction related to the interval with the lower limit $2R_{i-1}$ and the upper limit $2R_i$. The subscript

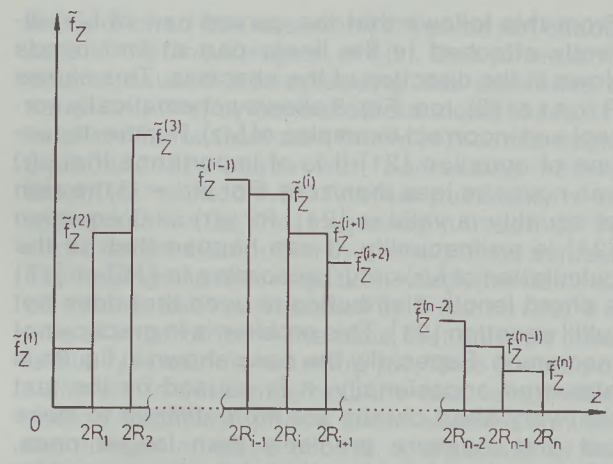

Fig. 7
Schematic description of a histogram of the chord length distribution used for the calculation of the particle size distribution

specifies the fraction (area fraction, fraction of the chord number, volume fraction):

$$\tilde{f}_Z^{(i)} = F_Z\left(2R_i\right) - F_Z\left(2R_{i-1}\right) \qquad [12a]$$

$$\tilde{f}_2^{(i)} = F_2\left(2R_i\right) - F_2\left(2R_{i-1}\right) \qquad [12b]$$

Equations [11], [12a] and [12b] lead to

$$\tilde{f}_2^{(i)} = \tilde{f}_Z^{(i)} + R_{i-1}\, f_Z\left(2R_{i-1}\right) - R_i\, f_Z\left(2R_i\right) \qquad [13]$$

The symbol $\tilde{f}_2^{(i)}$ stands for the area fraction of particles with diameters larger than $2R_{i-1}$ and smaller than $2R_i$. In [13] the value $\tilde{f}_Z^{(i)}$ is known from the measurement, for $f_Z(2R_i)$ the approximation

$$f_Z\left(2R_i\right) = \frac{d}{dz} F_Z(z)\Big|_{2R_i} \approx \frac{F_Z\left(2R_{i+1}\right) - F_Z\left(2R_{i-1}\right)}{2R_{i+1} - 2R_{i-1}} = \frac{\tilde{f}_Z^{(i+1)} + \tilde{f}_Z^{(i)}}{2R_{i+1} - 2R_{i-1}} \qquad [14a]$$

applying central differences is used. Special cases are:

$$f_Z\left(2R_1\right) = \frac{\tilde{f}_Z^{(2)} + \tilde{f}_Z^{(1)}}{2R_2} \qquad [14b]$$

$$f_Z\left(2R_n\right) = 0 \qquad [14c]$$

The equation [14c] is a consequence of [10]. From [11], [13] and [14a] to [14c] the following approximation $\tilde{f}_2^{*(i)}$ for $\tilde{f}_2^{(i)}$ can be deduced:

$$\tilde{f}_2^{*(1)} = \tilde{f}_Z^{(1)}\left(1 - \frac{R_1}{2R_2}\right) - \tilde{f}_Z^{(2)}\,\frac{R_1}{2R_2}$$

$$\tilde{f}_2^{*(2)} = \tilde{f}_Z^{(1)}\,\frac{R_1}{2R_2} + \tilde{f}_Z^{(2)}\left(1 + \frac{R_1}{2R_2} - \frac{R_2}{2(R_3 - R_1)}\right) - \qquad [15]$$

$$- \tilde{f}_Z^{(3)}\,\frac{R_2}{2(R_3 - R_1)}$$

$$\tilde{f}_2^{*(i)} = \tilde{f}_Z^{(i-1)}\,\frac{R_{i-1}}{2(R_i - R_{i-2})} + \tilde{f}_Z^{(i)}\left(1 + \frac{R_{i-1}}{2(R_i - R_{i-2})} - \right.$$

$$\left. - \frac{R_i}{2(R_{i+1} - R_{i-1})}\right) - \tilde{f}_Z^{(i+1)}\,\frac{R_i}{2(R_{i+1} - R_{i-1})} \qquad [15]$$

$$i = 3, 4, \ldots, n-1$$

$$\tilde{f}_2^{*(n)} = \tilde{f}_Z^{(n-1)}\,\frac{R_{n-1}}{2(R_n - R_{n-2})} + \tilde{f}_Z^{(n)}\left(1 + \frac{R_{n-1}}{2(R_n - R_{n-2})}\right)$$

The values $\tilde{f}_2^{*(i)}$ are sufficient information for a histogram that specifies the size distribution. The expected value $\bar{r}_2$ can most easily be calculated using [8] and does not demand the calculation of $\tilde{f}_2^{*(i)}$.

4.3.3. Determination of the distribution that is characterizing the volume fraction (frequency function $f_3(r)$)

The following calculations are based on a histogram of the chord length distribution and on equation [11]. According to [12a] and [12b]

$$\tilde{f}_3^{(i)} = F_3\left(2R_i\right) - F_3\left(2R_{i-1}\right) \quad i = 1, \ldots, n \qquad [16]$$

is the volume fraction of particles with diameters larger than $2R_{i-1}$ and smaller than $2R_i$. Similar to the procedure of section 4.3.2. the following approximation $\tilde{f}_3^{*(i)}$ for $\tilde{f}_3^{(i)}$ can be deduced from [5], [11] and [16]:

$$\tilde{f}_3^{*(1)} = \frac{1}{I}\left\{\tilde{f}_Z^{(1)}\left(R_1 - \frac{2}{3}\,\frac{R_1^2}{R_2}\right) - \tilde{f}_Z^{(2)}\,\frac{2}{3}\,\frac{R_1^2}{R_2}\right\}$$

$$\tilde{f}_3^{*(2)} = \frac{1}{I}\left\{\tilde{f}_Z^{(1)}\,\frac{2}{3}\,\frac{R_1^2}{R_2} + \tilde{f}_Z^{(2)}\left(R_1 + R_2 + \frac{2}{3}\,\frac{R_1^2}{R_2} - \right.\right.$$

$$\left.\left. - \frac{2}{3}\,\frac{R_2^2}{R_3 - R_1}\right) - \tilde{f}_Z^{(3)}\,\frac{2}{3}\,\frac{R_2^2}{R_3 - R_1}\right\}$$

$$\tilde{f}_3^{*(i)} = \frac{1}{I}\left\{\tilde{f}_Z^{(i-1)}\,\frac{2}{3}\,\frac{R_{i-1}^2}{R_i - R_{i-2}} + \tilde{f}_Z^{(i)}\left(R_{i-1} + \right.\right.$$

$$+ R_i + \frac{2}{3}\,\frac{R_{i-1}^2}{R_i - R_{i-2}} - \frac{2}{3}\,\frac{R_i^2}{R_{i+1} - R_{i-1}}\Big) - \qquad [17]$$

$$\left. - \tilde{f}_Z^{(i+1)}\,\frac{2}{3}\,\frac{R_i^2}{R_{i+1} - R_{i-1}}\right\} \quad i = 3, \ldots, n-1$$

$$\tilde{f}_3^{*(n)} = \frac{1}{I}\left\{\tilde{f}_Z^{(n-1)}\,\frac{2}{3}\,\frac{R_{n-1}^2}{R_n - R_{n-2}} + \right.$$

$$\left. + \tilde{f}_Z^{(n)}\left(R_n + R_{n-1} + \frac{2}{3}\,\frac{R_{n-1}^2}{R_n - R_{n-2}}\right)\right\}$$

In equation [17] the mean chord length $\bar{l}$ is used. It can be determined as the quotient of the total chord length within the phase under examination and the number of chords within this phase. If only a histogram of the cord length distribution is available it can be approximated by

$$\bar{l}^* = \sum_{j=1}^{n} \tilde{f}_Z^{(j)} \left(R_{j-1} + R_j\right) \qquad [18]$$

This approximation can be deduced under the simplification that the frequency function $f_Z(z)$ is constant in each chord length interval of the histogram.

Moreover the expected value $\bar{r}_3$ (cf. equation [6b]) is of interest. It can directly be calculated when the chord length distribution is known. For that purpose starting from equation [11] one can deduce:

$$\bar{r}_3 = \frac{2}{3} \frac{\int_0^{2r_{max}} \zeta^2 f_Z(\zeta)\, d\zeta}{\int_0^{2r_{max}} \zeta f_Z(\zeta)\, d\zeta} \qquad [19]$$

Using the same simplification as for equation [18] one gets the approximation

$$\bar{r}_3^* = \frac{8}{9} \frac{\sum_{j=1}^{n} \tilde{f}_Z^{(j)} \left(R_{j-1}^2 + R_j R_{j-1} + R_j^2\right)}{\sum_{j=1}^{n} \tilde{f}_Z^{(j)} \left(R_{j-1} + R_j\right)} \qquad [20]$$

As equation [18] shows the denominator of equation [20] can be replaced by $\bar{l}$ if it is known from the measurement.

4.4. Properties of the chord length distribution for spherical particles

The frequency function of the chord length distribution has some characteristic properties. The knowledge of these properties is helpful for the detection of errors in measurement. From equation [10] it is evident that the frequency function is linear for chord lengths less than $2r_{min}$. This linear part includes the origin. It should always appear because in all cases a smallest particle with a diameter larger then zero exists. But in practice it can happen that the linear part is not detectable, e.g. when the minimum particle size is below the upper limit of the smallest diameter intervall $2R_1$, or due to errors in measurement. Moreover by the help of equation [10] it can be shown that the frequency function $f_z(z)$ has to fulfill the condition

$$\frac{d}{dz} f_z(z) \leq \frac{f_Z(z)}{z} \qquad [21]$$

From this follows that the curved part of $f_Z(z)$ directly attached to the linear part at first bends down in the direction of the abscissa. This shows Richter (8), too. Fig. 8 shows schematically correct and incorrect examples of $f_Z(z)$. For the deduction of equation [21] it is of importance that $\mu(r)$ can never be less than zero. For $\mu(r) = 0$ the sign of equality is valid in [21], for $\mu(r) > 0$ equation [21] is an inequality. It can happen that for the calculation of $f_2(r)$ or $f_3(r)$ according to [15] or [17] a chord length distribution is used that does not fulfill equation [21]. This problem is in practice not incommon. Especially the case shown in fig. 8c is observed occasionally. It is caused by the fact that very short chords are more difficult to make out and measure precisely than longer ones. When such a chord length distribution is used for the determination of $f_2(r)$ or $f_3(r)$ negative values of $\tilde{f}_2^{*(i)}$ or $\tilde{f}_3^{*(i)}$ will occur in the region where [21] is not satisfied. In many cases the negative values only occur for the first few intervals, and their sum is very small. Then it can be assumed that errors in measurement only occur for very small chords, and the longer ones are measured sufficient precisely. In this case the error can be lessened. It is reasonable to replace the negative values by zero and then divide each of the positive values by the sum of all positive values, so that at last the sum of all values of $\tilde{f}_2^{*(i)}$ or $\tilde{f}_3^{*(i)}$ is unity again. It should

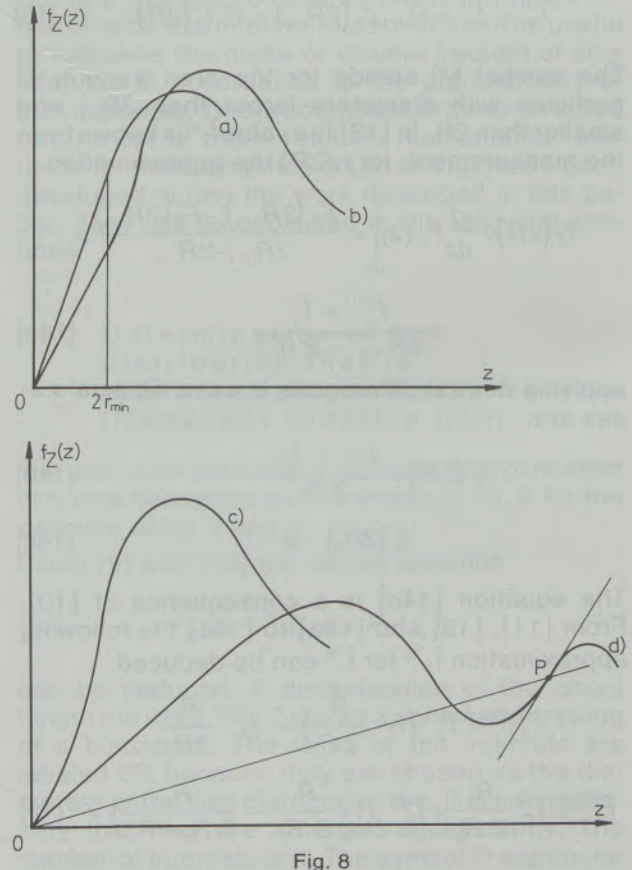

Fig. 8

Examples for a) correct and b), c), d) incorrect behaviour of $f_Z(z)$ (schematically)

be mentioned that equation [17] gives not exactly zero in the linear region of $f_Z(z)$. Due to the error that is caused by replaceing the derivative in equation [14a] by central differences it leads to a small deviation from zero that is in practice negligible and decreases with decreasing interval length (cf. section 4.5.). Another possibility is the approximation of the frequency function of the chord length distribution by a straight line containing the origin in the range of the negative calculated values, as it is proposed by Richter (8). It is also of importance in the case that only the mean radius $\bar{r}_2$ is calculated using [8]. Thus it would be sufficient to determine only the total length of all chords within the phase under examination and the number of these chords. A drawback of this method can be that it is not possible to estimate whether very short chords have been counted with too low frequency or not. Therefore it can even in this case be favourable to determine the chord length distribution. If necessary the above mentioned approximation of the frequency function of the chord length distribution can be applied and then the mean chord length $\bar{l}$ and the mean radius $\bar{r}_2$ can be calculated using equations [18] and [8]. In the case that too little of the small chord lengths have been counted the calculated value of $\bar{r}_2$ is without this correction too large.

4.5. Remarks on the numerical evaluation of chord length distributions

The equations [15], [17], [18] and [20] allow the calculation of approximations of the desired values. It is reasonable to demand that the error of the approximation approaches zero when the length of the intervals of the histogram that specifies the cord length distribution tends to zero at the same time.

With

$$h = \max_{i=1,\ldots,n} (R_i - R_{i-1}) \qquad R_0 = 0 \qquad [22]$$

the equations

$$\lim_{h\to 0} (\bar{r}_3^* - \bar{r}_3) = 0 \qquad [23]$$

$$\lim_{h\to 0} (\bar{l}^* - \bar{l}) = 0 \qquad [24]$$

should be valid. Contrary to that is the equation

$$\lim_{R_i - R_{i-1}\to 0} (\tilde{f}_m^{*(i)} - \tilde{f}_m^{(i)}) = 0 \qquad \begin{matrix} i = 1, \ldots, n;\ m = 2, 3 \\ R_0 = 0 \end{matrix} \qquad [25]$$

no sufficient condition for a satisfactory behaviour of $\tilde{f}_m^{*(i)}$ (m = 2, 3) because $\tilde{f}_m^{(i)}$ approaches zero itself for h → 0 as [12b] and [16] show. If the condition

$$\lim_{R_i - R_{i-1}\to 0} \frac{\tilde{f}_m^{*(i)} - \tilde{f}_m^{(i)}}{R_i - R_{i-1}} = 0 \qquad \begin{matrix} i = 1, \ldots, n;\ m = 2, 3 \\ R_0 = 0 \end{matrix} \qquad [26]$$

is satisfied, then

$$\lim_{R_{i-1}\to R_i} \frac{\tilde{f}_m^{*(i)}}{R_i - R_{i-1}} = f_m(2R_i) \qquad [27]$$

is valid. For a study of the error the following specification is used: an error g(h) is said to be of $O(h^k)$ (k is a positive integer) with the notation

$$g(h) = O(h^k) \qquad [28]$$

if in the vicinty of h = 0 the following equation is valid:

$$|g(h)| \le A \cdot |h^k| \qquad [29]$$

In [29] |g(h)| stands for the absolute value of g(h) and A for a positive constant. From this it is obvious how an upper limit for the absolute value of the error changes when h is varied. For the approximations $\bar{r}_3^*$ and $\bar{l}^*$ k should be at least unity, for $\tilde{f}_2^{*(i)}$ and $\tilde{f}_3^{*(i)}$ k ≧ 2 should be valid. This can be investigated by deducing the equations for $\tilde{f}_2^{*(i)}$, $\tilde{f}_3^{*(i)}$, $\bar{r}_3^*$ and $\bar{l}^*$ with the help of a Taylor series of $f_Z(z)$ (it is assumed that the Taylor series expansions used exist). The difference of the result of that method and the corresponding equations of the approximated values [15], [17], [18] and [20] is a power series expansion of the error. From this series $O(h^k)$ is evident. Fig. 9 shows the error $O(h^k)$ for the above-mentioned approximations deduced by this method. It is valid for equidistant spacing

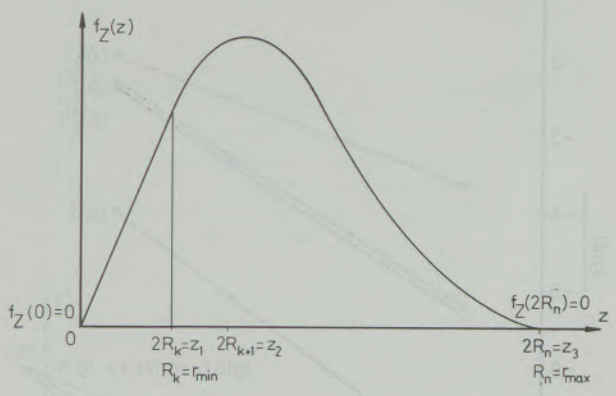

	all values of z except z_1, z_2, z_3	z_1, z_2	z_3
$\tilde{f}_2^{*(i)}, \tilde{f}_3^{*(i)}$	$O(h^3)$	$O(h^2)$ [1]	$O(h^2)$

$\bar{l}^*$	$O(h^4)$
$\bar{r}_3^*$	$O(h^2)$

[1] $O(h^2)$ is valid for $\mu(r_{min}) = 0$; $O(h)$ is valid for $\mu(r_{min}) > 0$

Fig. 9
Error $O(h^k)$ for the approximations used

of R_i; r_{min} and r_{max} coincide with values of R_i. As for $\tilde{f}_2^{*(i)}$ and $\tilde{f}_3^{*(i)}$ three special cases with $O(h^2)$ exist. Apart from this the error is $O(h^3)$. Special cases with an error $O(h^k)$ and $k > 3$ are possible when higher derivatives vanish; this is without significance for practical applications. So [26] and [27] are fulfilled. The footnote of fig. 9 mentiones a special case of O(h) that could appear for two radii and $\mu(r_{min}) > 0$. This does not seem to be a severe drawback. On the one hand the assumption of $\mu(r_{min}) = 0$ is a reasonable approximation for practical applications. On the other hand even in the case $\mu(r_{min}) > 0$ the error is limited to a diameter range that can be reduced by decreasing the length of the intervals. From Fig. 9 it can be seen that equations [23] and [24] are valid, too. An example for the behaviour of the error in the vicinty of h=0 shows fig. 10. This example is based on the distribution characterized by the functions shown in fig. 2 and 3. As the particle size distribution of this example was known the functions f_Z, $\tilde{f}_Z$, f_2, f_3, $\tilde{f}_2$ and $\tilde{f}_3$ as well as $\bar{l}$ and $\bar{r}_3$ could be calculated analytically. The analytically determined values of $\tilde{f}_Z$ have been used for the calculation of $\tilde{f}_2^*$, $\tilde{f}_3^*$, $\bar{l}^*$ and $\bar{r}_3^*$ by the help of equations [15],

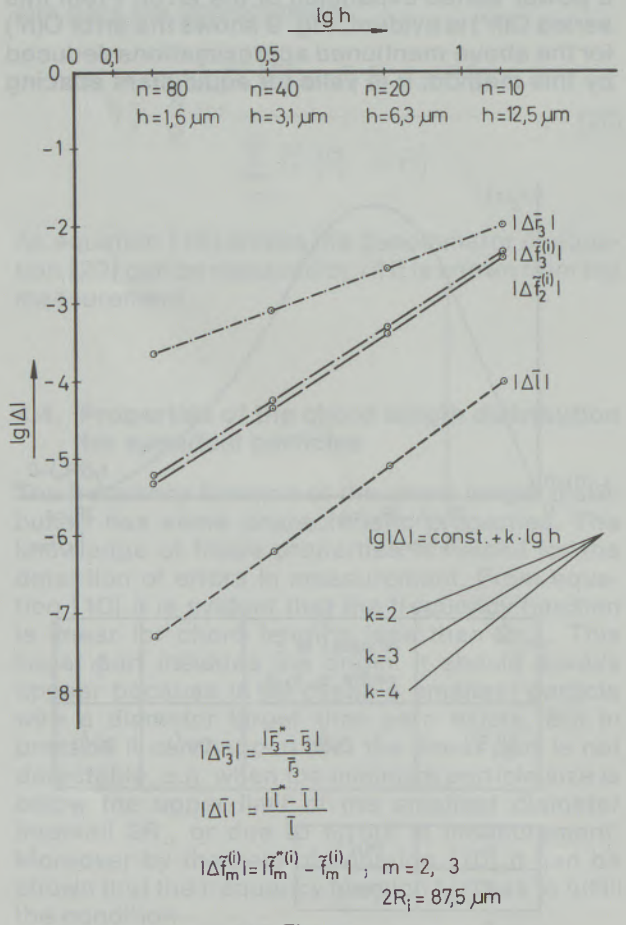

Fig. 10

Example for the behaviour of the error of the approximations used in the vicinity of h =0. The error is calculated for the size distribution shown in fig. 2 and 3

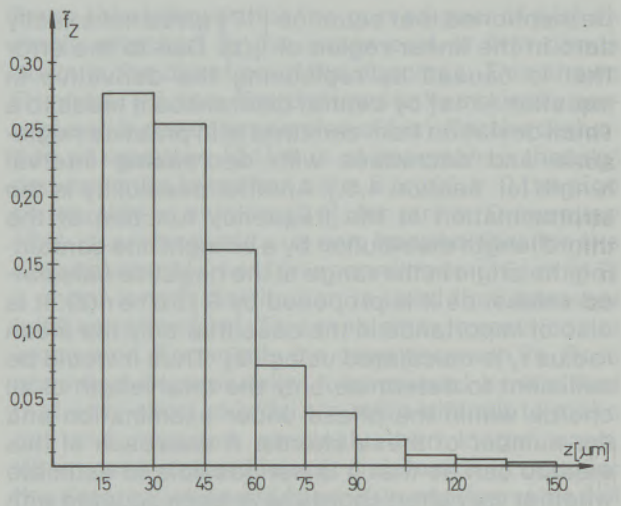

Fig. 11

Histogram of the chord length distribution of a sea-water magnesia; microscopical magnification 1000-times

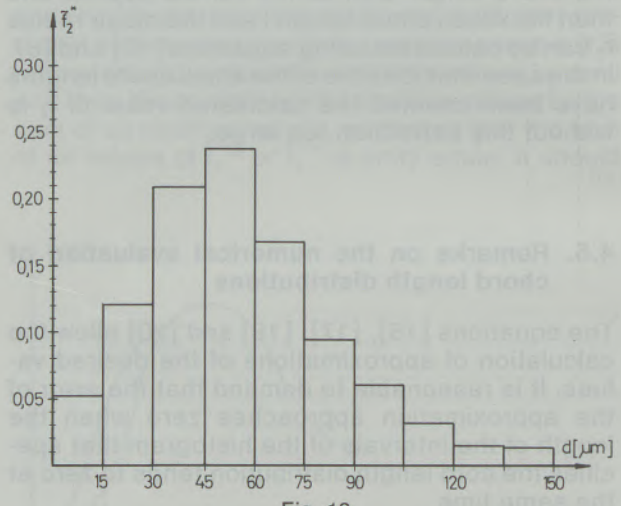

Fig. 12

Histogram $\tilde{f}_2^*$ (area fraction) calculated from fig. 11

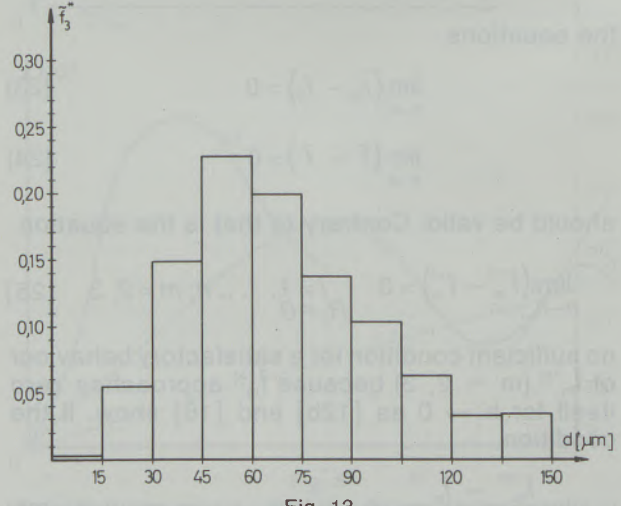

Fig. 13

Histogram $\tilde{f}_3^*$ (mass fraction) calculated from fig. 11

[17], [18] and [20]. For the denominator of equation [17] the approximation [18] has been used. The error was calculated using the analytical and the approximated values as spezified in fig. 10. This figure shows by the slope of the lines that the absolute value of an error $O(h^k)$ approaches for $h \rightarrow 0$ a function const · h^k. This example demonstrates the results of fig. 9. It has to be mentioned that the behaviour of the error in the vicinty of $h = 0$ is not always as simple as it appears in this case shown in fig. 10.

5. Examples

Fig. 11 shows a histogram ($\tilde{f}_z^{(i)}$) of the chord length distribution of a sea-water magnesia. Fig. 1c) shows a microphoto of that sample. The number of chords counted was 4000, the sum of all chord lengths approximately 149 mm. That gives a mean chord length $\bar{l}$ of 37 μm. The result of equation [18] is nearly identical. The mean diameter $\bar{d}_2$ calculated using equation [8] is 56 μm. Fig. 12 and 13 show $\tilde{f}_2^{*(i)}$ and $\tilde{f}_3^{*(i)}$. Using equation [20] the mean diameter $\bar{d}_3^* = 70$ μm can be calculated.

For the measurement discribed in fig. 11 a magnification of 1000-times was used. For demonstration of the error mentioned in section 4.4. the same polished section was investigated with a magnification of 180-times. Again 4000 chords have been counted. Fig. 14 shows $\tilde{f}_z^{(i)}$ for this second measurement. It can be seen that the first two intervals show the behavior of fig. 8c): because of the low magnification small chords have been measured in that case with too low frequency. That is why the mean chord length $\bar{l}$ is 42 μm and the mean diameter $\bar{d}_2$ 63 μm. From fig. 14 negative values for $\tilde{f}_2^{*(i)}$ and $f_3^{*(i)}$ would follow. Application of the correction mentioned in section 4.4. leads to the result discribed in fig. 15 and 16. The mean diameter $\bar{d}_3^*$ is 72 μm. Even the correction of Richter [8] mentioned in section 4.4. cannot compensate that error sufficiently. Applied on fig. 14 and using equation [18] it leads to $\bar{l} = 40$ μm and $\bar{d}_2 = 60$ μm. By comparison of both measurements it is evident that the correct magnification is of fundamental importance for the accuracy of the result. In this case the fatal error of the second measurement was deliberately caused for the sake of clarity.

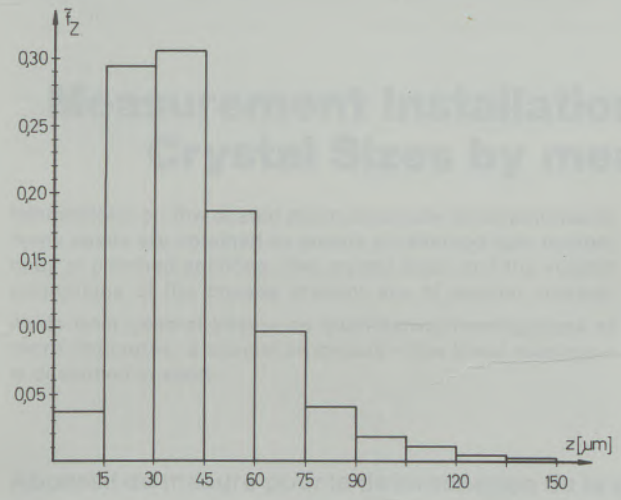

Fig. 14
Histogram of the chord length distribution of a sea-water magnesia; microscopical magnification 180-times

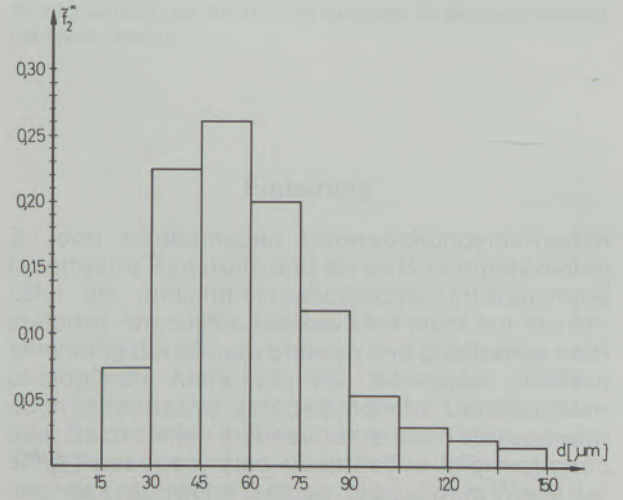

Fig. 15
Histogram $\tilde{f}_2^*$ (area fraction) calculated from fig. 14

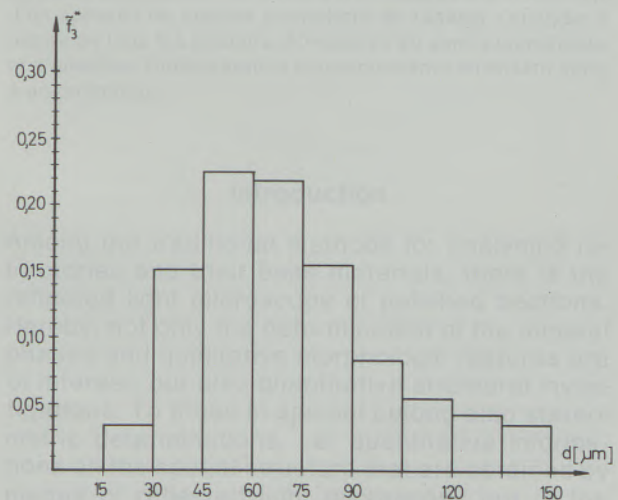

Fig. 16
Histogram $\tilde{f}_3^*$ (mass fraction) calculated from fig. 14

References/Literaturverzeichnis

1. Steinwender, W.: Measurement Installation for the Determination of Crystal Sizes by means of Lineal Analysis; Radex-Rdsch. **(1989)**, this issue, 183–191.
2. Quantitative Stereology – by E. E. Underwood/Addison Wesley Publishing Company: Reading **1970.**
3. Stereometrische Metallographie – by S. A. Saltykov/VEB Deutscher Verlag für Grundstoffindustrie: Leipzig **1974.**
4. Semler, C. E.: The Refractories of the People's Republic of China: An Advancing Industry; Ceramic Bulletin 68 **(1989)**, 1300–1305.
5. Oel, H. J.: Bestimmung der Größenverteilung von Teilchen, Kristalliten und Poren; Ber. DKG 43 **(1966)**, 624–631.
6. Exner, H. E.: Analysis of grain- and particle size distributions in metallic materials; Newsletter in Stereology **1973**, 111–128.
7. Tomandl, G.: A new method for calculating particle size distributions from chord and area distributions; Praktische Metallographie 16 **(1979)**, 413–419.
8. Richter, V.: Einige Verbesserungen des Verfahrens zur Ermittlung von Teilchengrößenverteilungen aus linearanalytischen Daten; Praktische Metallographie 17 **(1980)**, 157–170.
9. Spektor, A. G.: Particle size analysis of spherical particles in opaque substances (Russian); Zavod. Lab. 16 **(1950)**, 173–177.
10. Bockstiegel, G.: Eine einfache Formel zur Berechnung räumlicher Größenverteilungen aus durch Linearanalyse erhaltenen Daten; Z. Metallkde. 57 **(1966)**, 647–652.